Communication: A density functional investigation of structure-property evolution in the tetrakis hexahedral C4Al14 nanocluster

Benjamin J. Irving and Fedor Y. Naumkin

Citation: The Journal of Chemical Physics **141**, 131102 (2014); doi: 10.1063/1.4897259
View online: http://dx.doi.org/10.1063/1.4897259
View Table of Contents: http://scitation.aip.org/content/aip/journal/jcp/141/13?ver=pdfcov
Published by the AIP Publishing

Communication: A density functional investigation of structure-property evolution in the tetrakis hexahedral C_4Al_{14} nanocluster

Benjamin J. Irving[a] and Fedor Y. Naumkin[b]
Faculty of Science, University of Ontario Institute of Technology, 2000 Simcoe Street North, Oshawa, Ontario L1H 7K4, Canada

(Received 8 August 2014; accepted 24 September 2014; published online 6 October 2014)

Nanoclusters are prime objects of study in modern nanotechnology and offer a variety of applications promoted by their properties tunable by size, shape, and composition. DFT calculations are employed to analyze structure, stability, and selected electronic properties of a core-shell C_4Al_{14} species. With insertion of the carbon core, the original low-symmetry aluminum cluster is predicted to undergo a considerable reshaping and acquire a striking D_{4h} tetrakis-hexahedral geometry, with proportions controlled by a near-degenerate spin state or charge. The system also becomes more stable to dissociation. Surprisingly, other properties such as ionisation energy and electron affinity do not change significantly, although still exhibit some interesting features including opposite variations for vertical and adiabatic values. The stability and property evolutions are analyzed in terms of contributions from reshaping of the shell and its further interaction with the core. The system thus has potential applications as a symmetric building unit and a molecular device for nano-electronics/spintronics.
 [http://dx.doi.org/10.1063/1.4897259]

I. INTRODUCTION

Interest in nanoparticle design has shown unwavering growth throughout the past half-century.[1,2] This is primarily due to the fascinating properties exhibited by nanoparticles, distinct from those shown at the bulk and molecular level.[3–5] Although chemical composition naturally plays a crucial role in determining nanoparticle properties, size-manipulation is also of paramount importance in this regard, with perhaps the best known examples of size-dependent phenomena arising in quantum dots.[6,7] Different *shapes* can also be exploited in tuning nanoparticle properties. The conventional image tends to be that of a (roughly) spherical *core-shell* ensemble, although alternative shapes are now known to be important, particularly in light of their potential applications in diverse areas such as nanoelectronics and biomedical sensors.[8–11]

In our previous studies on core-shell C_nAl_{12} species, the $n = 4$ system has exhibited a unique behaviour. The original Al_{12} shell generally preserved its near-icosahedral structure for $n = 1$ to 3, but, apparently due to an "oversized" carbon core, acquired a tetracapped-cube-like geometry for C_4Al_{12}. In light of its unique structure, completing the shell of Al atoms that surround the C_4 core, by capping the two remaining faces of the Al_8 cage, is a tempting prospect as this allows us to verify if such a highly symmetric system could be stable and to investigate its properties. In addition, C_4Al_{14} has 58 valence electrons which is a "magic" number, suggesting an increased stability.[12]

Since the C_4Al_{14} system represents Al_{14} doped with C_4, it is interesting to check how different are its properties relative to those of Al_{14}, and to follow their evolution starting from the pure aluminum cluster. Previous *ab initio*[13] and mass spectral[14] studies have shown Al_{14} to exhibit *magic* behaviour. That is, upon adopting a capped-icosahedral geometry, the 3*s* electrons of the capping aluminum induce an electronic shell-closing effect, as in commonplace in metal clusters with 40 valence electrons (a "magic number" electron count coinciding with completion of the 2*p* electronic shell).

II. RESULTS

Initial calculations were aimed at identifying the (global) minimum of the neutral C_4Al_{14} nanocluster, as well as determining its electronic properties, namely, the (*vertical* and *adiabatic*) first ionisation potential, (V/A)IE_1, and electron affinity, (V/A)EA_1. Accordingly, the minimum energy geometries of the neutral, cationic, and anionic forms of the cluster have been calculated. Optimised conformations of the neutral cluster, for both the ground triplet state and near-degenerate singlet state, are presented in Figure 1, with key properties and parameters (of triplet) provided in Table I.

The central portion of the C_4Al_{14} cluster resembles a cyclic C_4 core, enclosed within an 8-membered aluminum "cuboid." Adjacent to each of the six faces of the cuboid sit the six remaining aluminum atoms. All C-C bonds are optimised to ~1.50 Å, and the C-Al bond lengths (considering immediate interactions only) lie within the range 2.19–2.28 Å (2.10–2.23 Å for the singlet state). The six "apical" aluminum atoms sit between 2.64 and 2.86 Å (cf. ~2.80 Å for short contacts and ~3.00 Å for long contacts of the singlet cluster) away from the four Al atoms comprising associated face of the Al_8 cuboid. All Al-Al bonds comprising the Al_8 structure are optimised to between 2.91 and 3.39 Å (2.76 and 3.40 for singlet).

[a]Benjamin.Irving@uoit.ca. Present address: Department of Control Engineering, Faculty of Electrical Engineering, Czech Technical University in Prague, Karlovo náměstí 13, 121 35 Prague 2, Czech Republic; email: irvinben@fel.cvut.cz.
[b]Fedor.Naumkin@uoit.ca

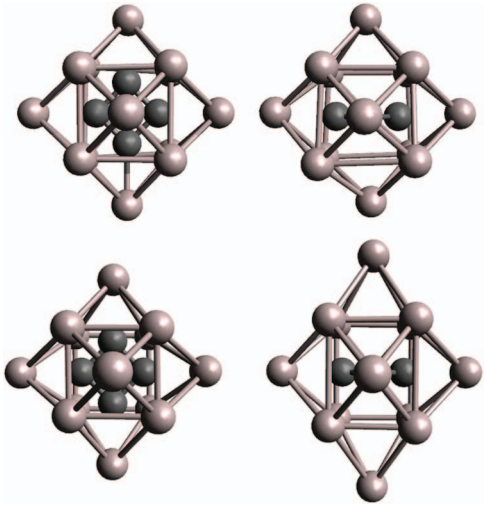

FIG. 1. Optimised minima for the C_4Al_{14} core-shell ensemble (C-Al bonds removed for clarity). Top row: Two projections of the ground triplet state. Bottom row: Two projections of the elongated singlet state cluster.

In the cationic form, $[C_4Al_{14}]^+$, the Al_8 cuboid is slightly more compact, now essentially consisting of two 4-membered rings of aluminum atoms, and slightly elongated perpendicular to the plane in which the C_4 ring resides. Both of the "Al_4" rings have all bonds optimised at ∼2.84 Å, with the longer edges optimised at ∼3.30 Å. As with the neutral cluster, all C-C bonds are optimised to ∼1.50 Å. Regarding the apical aluminum atoms, the shorter contact lengths are now ∼2.83 Å, with the longer ones ∼2.90 Å. The anionic form, $[C_4Al_{14}]^-$, has an even more distorted Al_8 cuboid at its core: two Al_4 rings with bonds optimised to an alternating pattern of ∼2.70 and ∼2.80 Å and an elongation (again perpendicular to the C_4 plane) of the longer cuboid edges to 3.50 Å. In this instance, the apical aluminum atoms are now somewhat more evenly dispersed, each lying between 2.80 and 2.90 Å away from their nearest neighbours.

Comparison of the D_e and D_e' values (defined in Sec. IV) shows that the overall interaction between the core and the shell contributes only ∼10% to the total stability of the system relative to C_4 + 14 Al. This is apparently due to a considerable restructuring of the aluminum shell. The singlet (S=0) and triplet (S=1) states of C_4Al_{14} are near-degenerate, with the triplet lying only ∼4 meV lower in energy than the singlet. Interestingly, the singlet state corresponds to a more "stretched" structure, as is evident in Figure 1. Besides, both D_e and D_e' values are lower than those for C_2Al_{12} studied by us previously, even though the latter species is not "magic." This is in accord with a similar situation for "magic" CAl_{12} and supports limited validity of the jellium model for clusters of mixed composition.

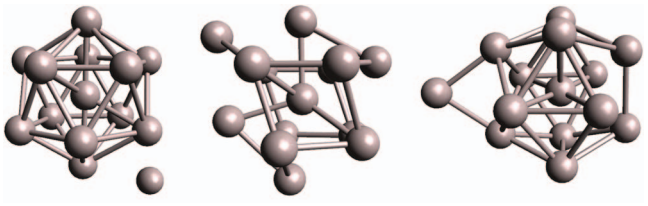

FIG. 2. L-R: Global minimum, Al_{14}^*; optimised minima of $[Al_{14}^*]^+$ and $[Al_{14}^*]^-$.

Additional calculations aimed at evaluating the comparative stabilities of the cationic and anionic forms of C_4Al_{14} have also been performed. Assuming, based on the relative IE and EA of the components,[15] we observe the following decomposition pathways: $[C_4Al_{14}]^+ \rightarrow C_4 + Al_{14}^+$ and $[C_4Al_{14}]^- \rightarrow C_4 + Al_{14}^-$. $[C_4Al_{14}]^+$ is apparently less stable than C_4Al_{14}, with a calculated D_e' of 3.88 eV (0.24 eV less than C_4Al_{14}). On the other hand, a negatively charged cluster is marginally more stable than its neutral counterpart, with $[C_4Al_{14}]^-$ having a D_e' of 4.15 eV (0.03 eV greater than C_4Al_{14}).

In previous calculations exploring the C_nAl_{12} (n = 1–4) series, for n = 4 we calculated a *vertical* first ionisation energy and electron affinity of 6.66 and 2.35 eV, respectively. The symmetrization of the cluster, as achieved *via* the addition of two aluminum atoms to form C_4Al_{14}, has not dramatically altered its electronic properties. We observe a 0.45 eV reduction (to 6.21 eV) in VIE_1, alongside a 0.18 eV increase (to 2.53 eV) in VEA_1. The *adiabatic* energies for C_4Al_{14} are similar to the vertical ones, suggesting that shape-change (or lack thereof) upon primary ionisation is not a defining factor in this instance.

In order to contextualize the properties of C_4Al_{14}, extensive calculations were performed on the "pure" Al_{14} cluster whose global minimum (denoted Al_{14}^*), alongside its ionic variants, are shown in Figure 2. Its structure is a capped, centrally occupied Al_{12} icosahedron, in which the core aluminum sits roughly 2.70 Å away from its surrounding atoms. The fourteenth Al atom assumes a position on the periphery of the cluster, equidistant (at 2.89 Å) from each of the three nearest Al atoms. This Al-Al contact length is only marginally longer than those found within the main body of the cluster, each of

TABLE I. Energetic and structural characterisation of C_4Al_{14} and all Al_{14} analogues. All values in eV and Å.

Cluster	D_e	D_e/m_{Al}	VIE_1	VEA_1	AIE_1	AEA_1	$R_e(Al-Al)$
C_4Al_{14}[a]	39.46	2.82	6.21	2.53	5.95	2.55	2.64–3.39
Al_{14}^*	35.35[b]	2.53	6.33	2.30	5.70	2.53	2.62–2.89
Al_{14}°	30.45[b]	2.18	5.98 (5.91)	2.72 (2.52)	n/a	n/a	2.76–3.00
$Al_{14}^\bullet$	35.32[b]	2.52	6.18	2.33	5.67	2.55	2.56–2.95

[a]For the C_4Al_{14} cluster, C-C bonds are all optimised to ∼1.50 Å; all C-Al interactions fall within the range 2.19–2.28 Å; $D_e' = 4.12$ eV.

[b]For each of the Al_{14} clusters, D_e essentially represents cluster binding energy in terms of the simple decomposition process: $Al_{14} \rightarrow 14Al$. Values in parentheses are for the singlet C_4Al_{14} case.

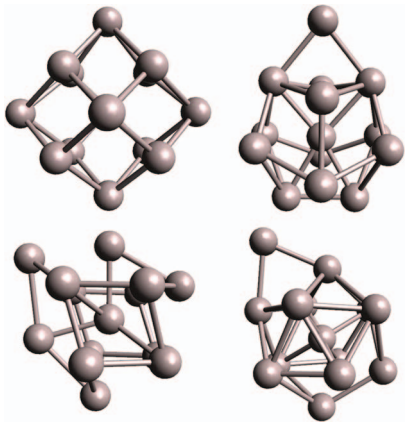

FIG. 3. Top row L-R: Structure of frozen shell (Al_{14}°) and optimised structure of $Al_{14}^{\bullet}$. Bottom row L-R: Optimised structures of $[Al_{14}^{\bullet}]^{+}$ and $[Al_{14}^{\bullet}]^{-}$.

which are approximately 2.75 Å. This is in good agreement with the previous investigations of Kumar.[13]

To complement the calculations performed on Al_{14}^{*}, we also studied the frozen Al_{14} shell of C_4Al_{14} (i.e., abstracting the Al coordinates from the neutral ground triplet state cluster shown in Figure 1 and performing single-point energy calculations for its neutral, cationic, and anionic forms) as well as the cluster obtained having (re)optimised the shell. The frozen shell and its optimised analogue will henceforth be denoted as Al_{14}° and $Al_{14}^{\bullet}$, respectively. The Al_{14}° shell is shown in Figure 3 (top left), along with the optimised neutral groundstate structure ($Al_{14}^{\bullet}$) and its (subsequently optimised) cationic and anionic forms.

Comparison of D_e values in Table I allows us to assign 9 eV (0.64 eV per Al atom) to the attractive interaction between the carbon core and aluminum shell in C_4Al_{14} (i.e., $D_e(C_4Al_{14}) - D_e(Al_{14}^{\circ})$). The binding in the shell is ~5 eV (0.35 eV/atom) weaker than in the relaxed aluminum cluster, consistent with longer Al-Al bonds.

Similar comparisons indicate the following differences in the property evolution. The VIE_1 value is slightly reduced when the aluminum cluster transforms into the shell, but then recovered with the further interaction (including charge transfer) with the core. By contrast, the VEA_1 value is first increased with inflating shell and then decreases by half as much (or remains, for the singlet state). Curiously, the corresponding AIE_1 and AEA_1 values exhibit opposite overall variations slightly increasing in the core-shell system relative to the pure aluminum cluster or staying same, respectively.

To gain further insight into the electronic structure of C_4Al_{14}, charge distribution within the cluster has also been studied. This entailed calculating Mulliken[16,17] and Löwdin[18] charges of C_4Al_{14} (triplet and near-degenerate singlet state) and its ions; the results are summarised in Table II. In general, it would appear that the C_4 core is insensitive to changes in cluster charge, with the comparatively electropositive formal charge borne by the Al_{14} shell exhibiting fluctuations in accord with charge and spin perturbations.

III. CONCLUSIONS

Density functional calculations predict a highly symmetric (D_{4h}) tetrakis-hexahedral geometry for the core-shell C_4Al_{14} nanocluster, very different from the original Al_{14} cluster (resembling an Al_{13} icosahedron with an additional "capping" Al atom). The C_4 core stabilizes the Al_{14} shell relative to dissociation, with the reduction of stability due to inflation of the shell more than compensated by the further core-shell interaction, including charge-transfer. When going from Al_{14} to C_4Al_{14}, the systems exhibit a considerable alteration of geometry but relatively weak variations of electronic properties such as vertical/adiabatic ionisiation energies and electron affinities. Insertion of the carbon core dramatically symmetrizes the aluminum shell. The weak evolution of these electronic properties in the sequence Al_{14}^{*} - $Al_{14}^{\bullet}$ - Al_{14}° - C_4Al_{14} indicates their low sensitivities to the Al_{14} geometry as well as the presence of C_4 inside. This illustrates the possibility of selective parameter variation, namely shaping the aluminum shell without affecting its electronic properties. Even though relatively weak, the variation in VEA_1 can be assigned predominantly to the inflation of the aluminum shell in the system. For VIE_1, however, the corresponding alteration is compensated for by the further interaction with the carbon core. Interestingly, upon relaxation of the ions, the net variations, for AEA_1 and AIE_1, interchange. In addition, the system exhibits a significant elongation upon transition into an ionic (both −/+) or near-degenerate singlet state. This exhibits a significant (inverted) property-structure relationship (property being charge- or spin-state) and might allow a nano-electronic/spintronic application as a charge- or spin-controlled switch.

IV. COMPUTATIONAL DETAILS

Calculations were performed at the DFT level employing the PBE0 functional and the 6-311g** basis set[19,20] on all atoms, as implemented in the NWChem *ab initio* software package.[21] Our benchmarking showed this combination of basis set and density functional to reproduce experimental parameters with suitable accuracy.[15,22] An overview of the performance of our method *vs* previous calculations and

TABLE II. Mulliken charges (χ^{M}) and Löwdin charges (χ^{L}) for the C_4Al_{14} cluster and its ions.

Cluster	χ_C^M	χ_{Al}^M	χ_C^L	χ_{Al}^L
C_4Al_{14}[a]	−0.77	−0.02 to +0.36	−0.31 to −0.30	−0.05 to +0.18
C_4Al_{14}[b]	−0.74	+0.11 to +0.24	−0.31	+0.06 to +0.13
$[C_4Al_{14}]^{+}$	−0.75	+0.21 to +0.30	−0.33	+0.14 to +0.22
$[C_4Al_{14}]^{-}$	−0.74 to −0.72	−0.01 to +0.17	−0.30	−0.07 to +0.04

[a]S = 1.
[b]S = 0.

experiment can be found in previous work.[23] Reasonable starting structures were generated using Avogadro.[24,25] All calculations were run on the *requin* node of the SHARCNET cluster.[26] For each system, the optimisation has been performed in a low symmetry, C_1, and energy minima confirmed *via* analysis of vibrational frequencies.

Both *vertical* and *adiabatic* first ionisation energies, (V/A)IE_1, and first electron affinities, (V/A)EA_1, are reported. Dissociation energies take into consideration the appropriate bond strengths (at 298 K): Al-Al ~167 kJ mol^{-1} (1.73 eV) < C-Al ~286 kJ mol^{-1} (2.96 eV) < C-C ~607 kJ mol^{-1} (6.29 eV).[15,27,28] Upon dissociation one may reasonably expect the carbon fragment to retain its structural integrity, whereas the partner aluminum cluster is atomized:

$$C_nAl_m \rightarrow C_n + m\text{Al}. \quad (1)$$

Alternatively, one is also likely to observe the less energetic scenario of the cluster being broken down into two separate clusters or "whole" constituent parts:

$$C_nAl_m \rightarrow C_n + Al_m. \quad (2)$$

This approach is in conformity with previous investigations.[29] All dissociation energies referring to Eqs. (1) and (2) are denoted as D_e and D'_e respectively. We also report D_e/m_{Al} values, i.e., the dissociation energy obtained *via* Eq. (1) per Al atom (in this instance, $m = 14$). Furthermore, all energies used for the calculations pertain to the lowest energy isomer obtained *via* our calculations (see the supplementary material).[30]

ACKNOWLEDGMENTS

We thank the Natural Sciences and Engineering Research Council of Canada (NSERC) for funding. Technical support of the staff of the SHARCnet academic HPC network of Ontario is gratefully acknowledged. Nous remercions le Conseil de Recherches en Sciences Naturelles et en Génie du Canada (CRSNG) pour le financement. Le support technique du personnel de SHARCnet (Réseau informatique de recherche académique hiérarchique et partagée) est grandement reconnu.

[1] R. G. Chaudhuri and S. Paria, Chem. Rev. **112**, 2373 (2012).
[2] J. Wang and X. C. Zeng, in *Nanoscale Magnetic Materials and Applications*, edited by J. P. Liu, E. Fullerton, O. Gutfleisch, and D. J. Sellmyer (Springer, 2009).
[3] L. D. Lloyd and R. L. Johnston, Chem. Phys. **236**, 107 (1998).
[4] C. Majumder, G. P. Das, S. K. Kulshrestha, V. Shah, and D. G. Kanhere, Chem. Phys. Lett. **261**, 515 (1996).
[5] E. Roduner, Chem. Soc. Rev. **35**, 583 (2006).
[6] V. I. Klimov, A. A. Mikhailovsky, S. Xu, A. Malko, J. A. Hollingsworth, C. A. Leatherdale, H.-J. Eisler, and M. G. Bawendi, Science **290**, 314 (2000).
[7] X. Michalet, F. F. Pinaud, L. A. Bentolila, J. M. Tsay, S. Doose, J. J. Li, G. Sundaresan, A. M. Wu, S. S. Gambhir, and S. Weiss, Science **307**, 538 (2005).
[8] W. Han, L. Yi, N. Zhao, A. Tang, M. Gao, and Z. Tang, J. Am. Chem. Soc. **130**, 13152 (2008).
[9] A. Radi, D. Pradhan, Y. Sohn, and K. T. Leung, ACS Nano **4**, 1553 (2010).
[10] L. Gou and C. J. Murphy, Nano Lett. **3**, 231 (2003).
[11] C.-C. Huang, Z. Yang, and H.-T. Chang, Langmuir **20**, 6089 (2004).
[12] Z. Luo, C. J. Grover, A. C. Reber, S. N. Khanna, and A. W. Castleman, Jr., J. Am. Chem. Soc. **135**, 4307 (2013).
[13] V. Kumar, Phys. Rev. B **57**, 8827 (1998).
[14] M. F. Jarrold, J. E. Bower, and J. S. Kraus, J. Chem. Phys. **86**, 3876 (1987).
[15] NIST Chemistry WebBook, see http://webbook.nist.gov/chemistry/ (2011); accessed 23 July 2013.
[16] R. S. Mulliken, J. Chem. Phys. **23**, 1833 (1955).
[17] R. S. Mulliken, J. Chem. Phys. **23**, 1841 (1955).
[18] P. O. Löwdin, Adv. Quantum Chem. **5**, 185 (1970).
[19] A. D. McLean and G. S. Chandler, J. Chem. Phys. **72**, 5639 (1980).
[20] R. Krishnan, J. S. Binkley, R. Seeger, and J. A. Pople, J. Chem. Phys. **72**, 650 (1980).
[21] M. Valiev, E. J. Bylaska, N. Govind, K. Kowalski, T. P. Straatsma, H. J. J. V. Dam, D. Wang, J. Nieplocha, E. Apr, T. L. Windus, and W. A. de Jong, Comput. Phys. Commun. **181**, 1477 (2010).
[22] C. R. Brazier, J. Chem. Phys. **98**, 2790 (1993).
[23] B. J. Irving and F. Y. Naumkin, Phys. Chem. Chem. Phys. **16**, 7697 (2014).
[24] M. D. Hanwell, D. E. Curtis, D. C. Lonie, T. Vandermeersch, E. Zurek, and G. R. Hutchison, "Avogadro: An advanced semantic chemical editor, visualization, and analysis platform," J. Chemoinf. **4**, 17 (2012).
[25] Avogadro: An open-source molecular builder and visualization tool, Version 1.1.0, see http://avogadro.openmolecules.net/.
[26] SHARCNET, see https://www.sharcnet.ca/ for an overview of the high performance computing facilities provided by the SHARCNET consortium.
[27] B. deB. Darwent, *Bond Dissociation Energies in Simple Molecules* (U.S. National Bureau of Standards, Washington; for sale by the Superintendent of Documents, United States Government Printing Office, 1970).
[28] Y.-R. Luo, *Handbook of Bond Dissociation Energies in Organic Compounds* (CRC Press, 2002).
[29] F. Y. Naumkin, J. Chem. Phys. A **112**, 4660 (2008).
[30] See supplementary material at http://dx.doi.org/10.1063/1.4897259 for Cartesian coordinates and energies of the optimised geometries.